5B

Preprint
RAL-P-96-002

Determining Mixed Linear-nonlinear Coupled Differential Equations From Multivariate Time Series Data

A D Irving and T Dewson

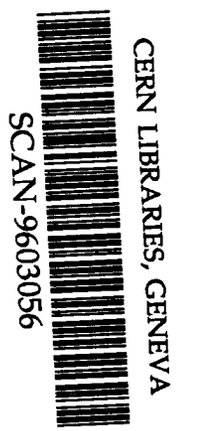

Sw9611

February 1996

COUNCIL FOR THE CENTRAL LABORATORY OF THE RESEARCH COUNCILS

The Central Laboratory of the Research Councils
Library and Information Services
Rutherford Appleton Laboratory
Chilton
Didcot
Oxfordshire
OX11 0QX
Tel: 01235 445384 Fax: 01235 446403
E-mail library@rl.ac.uk

ISSN 1361-4762

Neither the Council nor the Laboratory accept any responsibility for loss or damage arising from the use of information contained in any of their reports or in any communication about their tests or investigations.

Determining mixed linear-nonlinear coupled differential equations from multivariate time series sequences

A D Irving[+] and T Dewson*

[+] Rutherford Appleton Laboratory, Chilton, Didcot, Oxon, OX11 OQX, UK.
* Dept of Mathematics, The University of Bristol, University Walk, Bristol BS8 1TW, UK.

Abstract

A new method is described for extracting mixed linear-nonlinear coupled differential equations from multivariate time series data. A tractable hierarchy of moment equations is generated by operating on a suitably truncated Volterra functional expansion. The hierarchy facilitates the calculation of the coefficients of the coupled differential equations. In order to demonstrate the methods ability to accurately estimate the coefficients of the governing differential equations the method is applied to data derived from the numerical solution of the Lorentz equations with additive noise. The method is then used to construct a dynamic global mid- high-magnetic latitude ionospheric model. It is shown that the estimated inhomogeneous coupled second order differential equation model for the ionospheric fof2 peak plasmas density can accurately and consistently forecast the future behaviour of the ionosphere for a set of ionosonde stations which encompass the earth at mid-and high magnetic latitudes. The hierarchy method can be used to characterise the observed behaviour of a wide class of coupled linear and mixed linear-nonlinear phenomena.

Introduction

The complex nature of the time series sequences of coupled nonlinear processes renders their quantitative analysis extremely difficult in general. This is partially because the mapping between adjacent members of each time series sequence is nonlinear but also because the multivariate relationships are functions of many stochastic or chaotic variables. The main concern of the study of physical phenomena is to establish the causal deterministic relationships which characterise a given set of physical observables. Each mathematical representation chosen to underpin the empirical relationship is inevitably dependent on the experimental establishment of reproducible, accurate and consistent coefficients which characterise the phenomena. Without these coefficients the findings of numerical and analytical studies generally remain qualitative. There is thus a need to develop and refine data analysis methods which can calculate coefficients suitable for incorporation into the mathematical representation that provides a rigorous, unambiguous and quantitative description within a specified range of accuracy.

For many physical processes the causal relationship between the physical observables can be represented as coupled nonlinear partial differential equations. One general way to 'invert' coupled single valued coupled differential equations is by using the Volterra functional expansion [1]. The solution of the differential equations is considered to be composed of an ascending order functional expansion. This inverse form of differential equations can be used to analyse the time series data from a wide class of physical phenomena and time invariant examples are presented elsewhere [2-5].

Evolutionary input-output processes are dependent on the temporal derivatives of the input physical observables of the vector valued process which is assumed to be T th order differentiable and the inverse form can be used [6].

In this work the behaviour of the vector valued process is represented as a set of coupled ordinary differential equations of the form

$$\sum_{k=0}^{K} a_k \frac{d^k x_i(t)}{dt^k} = F_i\left(x_1,\ldots,x_M, \frac{dx_1}{dt},\ldots,\frac{dx_M}{dt},\ldots,\frac{d^T x_1}{dt^T},\ldots,\frac{d^T x_M}{dt^T} \right) \qquad (1)$$

In dynamical system theory it is assumed that T=(K-1) and that the first degree differential equation in its highest power can be written as

$$\frac{d^K x_i(t)}{dt^K} = \Im_i\left(x_1,\ldots,x_M, \frac{dx_1}{dt},\ldots,\frac{dx_M}{dt},\ldots,\frac{d^{K-1} x_1}{dt^T},\ldots,\frac{d^{K-1} x_M}{dt^T} \right) \qquad (2)$$

This form can always be reduced to an equivalent set of coupled first order ordinary differential equation form with

$$\frac{d^K x_i(t)}{dt^K} = G_i(x_1,\ldots,x_M) \tag{3}$$

The coupled first order ordinary differential equation representation has been used to associate topological structures with experimental time series [7,8]. For example many physical laws are expressed in infinitesimal form with the corresponding differential equations being defined as a vector field. A vector field in this case is interpreted as the right hand side of the coupled ordinary differential equations given by equation (3) which are satisfied by the integral curves denoted by the time series trajectories $\{x(t)\}$. The form of equation (3) facilitates the 'reconstruction' of a set of differential equations in phase space which mimic some aspects of the phenomena. There have been a number of previous attempts to extract from time series data coupled differential equations which replicate aspects of the observed behaviour [9-16].

In this work, particular emphasis is placed on characterising complex behaviour in the context of coupled differential equations. A new method for extracting coupled mixed order linear-nonlinear differential equations from time series data in the presence of noise is developed. The method employs the hierarchy moment formalism to characterise the mapping between time series values [17]. The coefficients of the coupled differential equations are estimated with the hierarchy moment method.

The method developed in this work is first applied to data derived from the numerical solutions of the much studied Lorentz equations. This numerical example is used to demonstrate the accuracy and appropriate use of the method. Then, as an example application, the method is applied to the analysis of time series ionosonde measurements collected simultaneously around the earth at mid- and high- magnetic latitudes. In particular, an empirical model of the global fof2 ionospheric maximum plasma density is developed and used to predict the rolling out of sample future behaviour. This is the first empirical model which can accurately predict the future dynamical global behaviour of the ionospheric fof2. The model developed is based on a set of coupled inhomogeneous second order nonlinear differential equations.

An accurate and consistent empirical model of the ionosphere would help resolve a number of outstanding theoretical and practical geophysical problems [18]. In addition, it would facilitate the verification of available theoretical simulation models where agreement presently remains qualitative in form [19,20].

The hope and expectation is that empirical forecasts can be used to provide more realistic boundary conditions for available global theoretical ionospheric-thermospheric models. Not only will this increase the practical limit for out of sample spatial and temporal predictions of observed behaviour, but they may further the understanding of the physical mechanisms which produce the observed plasma distributions in the earth's upper atmosphere. The application of empirical coupled differential equation models to the verification of global ionospheric-thermoshperic simulation models will be discussed in detail elsewhere.

A Volterra functional representation of coupled differential equations

Consider the set of coupled simultaneous differential equations given by

$$\sum_{k=0}^{K} a_k \frac{d^k x_i(t)}{dt^k} = F_i\left(x_1,\ldots,x_M,\frac{dx_1}{dt},\ldots,\frac{dx_M}{dt},\ldots,\frac{d^T x_1}{dt^T},\ldots,\frac{d^T x_M}{dt^T} \right)$$

where it is assumed that the vector sequence has temporal derivatives that exist up to order T. Assume that the coupled equations have an inverse solution defined by

$$x_i(t) = G_i\left(x_1,\ldots,x_M,\frac{dx_1}{dt},\ldots,\frac{dx_M}{dt},\ldots,\frac{d^T x_1}{dt^T},\ldots,\frac{d^T x_M}{dt^T} \right) \tag{4}$$

and has the temporal derivatives to order T of the form

$$\frac{d^k x_i(t)}{dt^k} = H_i\left(x_1,\ldots,x_M,\frac{dx_1}{dt},\ldots,\frac{dx_M}{dt},\ldots,\frac{d^T x_1}{dt^T},\ldots,\frac{d^T x_M}{dt^T} \right) \tag{5}$$

Most physical processes evolve, and evolve only under the influence of external processes and their temporal derivative. Although such processes display auto-regressive attributes, the evolution will normally cease when the external stimuli stop. For these situations the evolution of the physical process will be a multivariate function of a total of N independent physical observables and their temporal derivatives. The relationship between the element of the physical observables can be written as an ascending multivariate Taylor series expansion.

Equally, the phenomena can be described by an expansion of functionals which characterises the physical process as a mapping between functional spaces.

If there is a unique solution to the Taylor series expansion then, formally at least, it is the inverse mapping. The emphasis of the inverse problem approach is to identify the form of relationship between the observables and hence establish the laws governing the process. If the physical processes responds in a finite time, say μ units, then the nonlinear behaviour of a physical observables and its temporal derivatives can be represented as a discrete Volterra functional expansion truncated to order N, defined by

$$\phi_{u_v}(t) = \sum_{n=1}^{N} \frac{1}{n!} \sum_{i_1=1}^{M} \cdots \sum_{i_n=i_n-1\sigma_1=0}^{M} \sum_{\sigma_n=0}^{\mu} \cdots \sum_{\sigma_n=0}^{\mu} h_{\phi_{u_v}\Phi_{i_1}\ldots\Phi_{i_n}}(\sigma_1,\ldots,\sigma_n)$$
$$\prod_{j=1}^{n} \Phi_{i_j}(t-\sigma_j)\,\delta\left(u_v \neq i_j;\ u_v = i_j\ \sigma_j > 0\ j=1,\ldots,n\right) \qquad (6)$$

where N is the order of truncation of the Volterra functional expansion, T is the highest order of temporal derivative considered, t denotes time, the σ_js denote time delay with respect to the time t and the delta function denotes the fact that lower limit for each auto-regressive sum over each index value u_v start from 1, whilst all the other summations start from 0.

. Here the elements $\phi_{u_v}(t)$ are drawn from the set of physical observables $\{\phi_u(t)\} = \left\{x_u, \frac{dx_u}{dt}, \ldots, \frac{d^T x_u}{dt^T}\right\}$ and the elements $\Phi_{i_j}(t)$ are drawn from the set of physical observables $\{\Phi_i(t)\} = \left\{x_1, \ldots x_M, \frac{dx_1}{dt}, \ldots, \frac{dx_M}{dt}, \ldots, \frac{d^T x_1}{dt^T}, \ldots, \frac{d^T x_M}{dt^T}\right\}$.

The kernel function values $h_{\phi_{u_v}\Phi_{i_1}\ldots\Phi_{i_n}}(\sigma_1,\ldots,\sigma_n)$ characterise the behaviour. The discrete, truncated Volterra series remains ill posed in the sense that there are too many unknown coefficients to solve for. Thus, the approximate method of discretisation used for the linear case cannot by themselves be used to solve the Volterra series. In addition, as time series sequences of physical observables are generally stochastic in form, the equations are also ill conditioned.

The conditioning can be improved by statistical averaging and the use of operators allows a set of tractable equations with average variable values to be generated. For each Volterra series expansion, a tractable set of simultaneous equations with well behaved coefficients can be generated by taking time series moments of a suitably truncated Volterra series expansion.

Each separate equation is operated on with a series of averaging operators, one for each permutation of delayed variables $\left\langle \prod_{r=1}^{R} \Phi_{i_r}(t-\tau_r)* \right\rangle$, where $i_r = 1,\ldots,\pi$ to give the set of moment hierarchies defined by

$$\left\langle \prod_{r=1}^{R} \Phi_{k_r}(t-\tau_r)\phi_{u_v}(t) \right\rangle = \sum_{n=1}^{N} \frac{1}{n!} \sum_{i_1=1}^{M} \cdots \sum_{i_n=i_{n-1}\sigma_1=0}^{M} \sum^{\mu} \cdots \sum_{\sigma_n=0}^{\mu}$$

$$h_{\phi_{u_v}\Phi_{i_1}\ldots\Phi_{i_n}}(\sigma_1,\ldots,\sigma_n)$$

$$\left\langle \prod_{r=1}^{R} \Phi_{k_r}(t-\tau_r) \prod_{j=1}^{n} \Phi_{i_j}(t-\sigma_j)\delta\left(u_v \neq i_j;\ u_v = i_j\ \sigma_j > 0 \quad j=1,\ldots,n\right) \right\rangle \qquad (7)$$

The moment hierarchy can be rewritten in the obvious matrix form $\underline{C} = \underline{\underline{M}}\underline{h}$. Here $\underline{\underline{M}}$ is a square matrix whose elements are the ascending order auto-moments of the multivariate time series data and their temporal derivatives. For each moment hierarchy $\underline{C}$ is a column vector whose elements are the ascending order cross-moments of the multivariate time series data and their temporal derivatives. The elements of the column vector $\underline{h}$ are the unknown kernel function values. If the matrix $\underline{\underline{M}}$ is non-singular then $\underline{h} = \left(\underline{\underline{M}}\right)^{-1}\underline{C}$ has a unique solution. Given the properties of typical time series data and construction of the moment values used in the moment hierarchy, the rows of $\underline{\underline{M}}$ will be linearly independent of each other, thus the matrix will be non-singular and have a unique solution. This will be the case for many mixed stochastic and deterministic processes.

The effect of noise and uncertainty in experimental data

Whilst the mathematics of models is precise the models themselves are not. Models are only approximations to the complex behaviour observed in the real world and are based on the empirical measurement of physical observables. Each individual empirical measurement is limited in its precision due to stochastic fluctuations in the physical observable and in the sensor used to measure it and the finite accuracy to which each sensor can be calibrated. The stochastic fluctuations give rise to a replication uncertainty when the same apparatus in the same experimental design.

The calibration uncertainty is partially due to the ability to maintain the physical condition of fixed point values, for example the melting point of a solid, and partially due to the interpolation of the sensors nonlinear response between fixed calibration points. The calibration uncertainty is usually much larger than the stochastic uncertainty and it is important to consider both when comparing the findings of different observations of the same phenomena.

Generally speaking, empirical measurements are made in order to confirm or to disprove a hypothesis or theory. The physical quantities which underpin the theory, such as parameters or fundamental constants, are not directly measurable in themselves, but must be derived from the observational data. If the uncertainty aspects of the problem are neglected then theoretical considerations provide a framework for the manipulation of the data in order to obtain the values of the desired quantities. Having established the value of the parameters of the theoretical representation it is necessary to consider their uncertainty. This is achieved through the theory of propagation of uncertainty which can either be applied during the parameter estimation process or independently of it.

The observed physical values $\{\phi_u(t)\} = \left\{x_u, \frac{dx_u}{dt}, \ldots, \frac{d^T x_u}{dt^T}\right\}$ are considered to be composed of an additive component of stochastic noise and a deterministic component. The stochastic component of the uncertainty which is often thought of as 'noise' on the observation values. The deterministic component can be analysed and used to predict the future behaviour of the phenomena. Each time series value of the physical observables is theoretical decomposed into a deterministic component and a stochastic component and this introduces additional variables into the representation.
Each element of the sequence of data $\{\phi_u(t)\}$ can be written as

$$\begin{aligned}\phi_{u_v}(t) &= \Xi_u(t) + \theta_{u_v}(t) \\ &= \Xi_u(t) + \sum_{n=1}^{N} \frac{1}{n!} \sum_{i_1=1}^{M} \cdots \sum_{i_n=i_{n-1}\sigma_1=0}^{M} \sum_{\sigma_n=0}^{\mu} \cdots \sum_{\sigma_n=0}^{\mu} h_{\phi_{u_v}\Phi_{i_1}\ldots\Phi_{i_n}}(\sigma_1,\ldots,\sigma_n) \\ &\prod_{j=1}^{n} \left\{\Phi_{i_j}(t-\sigma_j) - \Xi_{i_j}(t-\sigma_j)\right\} \delta\left(u_v \neq i_j;\ u_v = i_j\ \sigma_j > 0\ \ j=1,\ldots,n\right)\end{aligned} \tag{8}$$

In the present work $\{\Xi_k(t)\}$ are assumed to be drawn from Gaussian random processes so that estimates for their variance can be obtained, for example, by regression or maximum likelihood methods. This enables the kernel function values to be determined from the moment hierarchies [2-6]. The kernel, or response, function values are then used to predict the out of sample behaviour of the phenomena being studied.
Obviously, the estimated response function values, or mappings, $h_{\phi_{u_v}\Phi_{i_1}\ldots\Phi_{i_n}}(\sigma_1,\ldots,\sigma_n)$ are dependent on the choice of $\{\Xi_k(t)\}$. This is also true for other representations that decompose the data into separate deterministic and stochastic components.
Such representations, in general, are non-unique characterisations of the data and are not likely to yield detailed quantitative insight into the physics underlying the process.

Operating on the Volterra series with the averaging operator $\left\langle \prod_{r=1}^{R} \Phi_{i_r}(t-\tau_r)* \right\rangle$ the R th order absolute moment equation is, after re-arrangement [17], by definition

$$\left\langle \prod_{r=1}^{R} \Phi_{i_r}(t-\tau_k)\phi_{u_v}(t) \right\rangle = \left\langle \prod_{r=1}^{R} \Phi_{i_r}(t-\tau_k)\Xi_u(t) \right\rangle$$
$$+ \sum_{n=1}^{N} \frac{1}{n!} \sum_{i_1=1}^{M} \cdots \sum_{i_n=i_n-1\sigma_1=0}^{M} \sum^{\mu} \cdots \sum_{\sigma_n=0}^{\mu} h_{\phi_{u_v}\Phi_{i_1}\ldots\Phi_{i_n}}(\sigma_1,\ldots,\sigma_n)$$
$$\delta\left(u_v \neq i_j;\ u_v = i_j\ \sigma_j > 0\ \ j=1,\ldots,n\right)$$
$$\left\langle \prod_{r=1}^{R} \Phi_{i_r}(t-\tau_k) \prod_{j=1}^{n} \left\{ \Phi_{i_j}(t-\sigma_j) - \Xi_{i_j}(t-\sigma_j) \right\} \right\rangle \qquad (9)$$

The moment hierarchy form given by equation (9) can readily be solved for the unknown noise coefficients $\{\Xi_k(t)\}$ using , for example, regression or maximum likelihood methods [17].

The application of averaging operators to the Volterra series has transformed the vector nonlinear polynomial expansion into a simple algebraic form by generating a hierarchy of tractable moment equations with well behaved coefficients. This moment hierarchy is then regressed to obtain the variance of the noise and the unknown response function values. Given that the choice of $\{\Xi_k(t)\}$ is not unique, it is assumed here that $\{\Xi_k(t)\}$ is drawn from a zero mean Gaussian white noise process which is statistically independent to the deterministic components $\{\varphi_u(t)\}$.

The moment hierarchy has the obvious linear algebraic form

$$\underline{\Psi} = \underline{\underline{\Psi}}\,\underline{h} \qquad (10)$$

where the cross - moment elements are given by

$$\Psi_R(\tau_1,\ldots,\tau_R) = \left\langle \prod_{r=1}^{R} \Phi_{i_r}(t-\tau_k)\,\phi_{u_v}(t) \right\rangle$$

the off block - diagonal auto - moment elements are given by

$$\Psi_{Rn}(\tau_1,\ldots,\tau_R,\sigma_1,\ldots,\sigma_n) = \alpha_{Rn}\left\langle \prod_{r=1}^{R} \Phi_{i_r}(t-\tau_k)\prod_{j=1}^{n} \Phi_{i_j}(t-\sigma_j)\right\rangle$$

the off block - diagonal auto - moment elements are given by

$$\Psi_{RR}(\tau_1,\ldots,\tau_R,\sigma_1,\ldots,\sigma_R) = \beta_{RR}\left\langle \prod_{r=1}^{R} \Phi_{i_r}(t-\tau_k)\prod_{j=1}^{R} \Phi_{i_j}(t-\sigma_j)\right\rangle - \gamma^R$$

and the response function elements are $h_{\phi_{u_v}\Phi_{i_1}\ldots\Phi_{i_M}}(\sigma_1,\ldots,\sigma_M)$.

The variance of the stochastic component is denoted as γ, and the coefficients α_{Rn} and β_{RR} reflect the fact that the symmetry of the equations has been used to reduce the order of the matrix [17].

Now consider the effect of the uncertainty on the experimental measurements. In accordance with standard uncertainty analysis of experimental data, assume that it is possible for the analysis procedure to yield a unique set of empirical coefficients, that are physically meaningful, and where each coefficient has an uncertainty value associated with it.

Including the uncertainty terms the moment hierarchy retains a linear algebraic form with

$$(\underline{\psi} \pm \underline{\Delta\psi}) = (\underline{\underline{\Psi}} \pm \underline{\underline{\Delta\Psi}})(\underline{h} \pm \underline{\Delta h}) \tag{11}$$

Using the theory of the propagation of errors the fractional error on the estimated mixed order linear-nonlinear response function values will be given by

$$\frac{|\underline{\Delta h}|}{|\underline{h}|} \le C(\underline{\underline{\Psi}})\left[\frac{\|\underline{\underline{\Delta\Psi}}\|}{\|\underline{\underline{\Psi}}\|} + \frac{|\Delta\psi|}{|\psi|}\right] \tag{12}$$

where $\|\ \|$ denotes the norm and the conditioning number is defined as $C(\underline{\underline{\Psi}}) = \|\underline{\underline{\Psi}}\| \bullet \|\underline{\underline{\Psi}}^{-1}\|$.

These uncertainty values can be used to estimate the standard error, and multiples thereof, of the forecasted physical observables.

Thus the moment hierarchy method provides not only the a values for the future behaviour of each of the coupled physical observable but also it provides a probability distribution associated with each forecast.

Numerical example of the Lorentz coupled nonlinear differential equations

In this section the results from a numerical experiment are presented where the properties of the nonlinear system are known. A numerical experiment is used in which the accuracy and range of appropriate use for the method in estimating the nonlinear response values and the ability to predictive the future behaviour are assessed.

The example chosen is the widely used Lorentz equations, which are a set of low order coupled nonlinear differential equations which describe the dynamical behaviour of convective motion in the atmosphere, with

$$\frac{dx_1}{dt} = -Px_1 + Px_2$$
$$\frac{dx_2}{dt} = -x_1x_3 + Rx_1 - x_2$$
$$\frac{dx_3}{dt} = x_1x_2 - Dx_3$$

where x1(t) is a coefficient of the stream function of the fluid, x2(t) is a mixed horizontal and vertical component of the temperature gradient, x3(t) is a vertical component of the temperature gradient in the fluid, P is the Prandtl number, R is the Reynolds number of the fluid and D is a measure of the energy dissipation within the fluid. For P>D+1 the convective motion is unstable when R>24.74. For values of Reynolds number satisfying this inequality the coupled ordinary differential equations exhibit a strange attractor with two steady states between which the trajectory oscillates. The values used in this numerical example are P=10.0, R=100.8 and D=8/3.

The data sequences were generated using the above equation and some 50000 points of data in each sequence were generated. However, only 500 of the data points in each sequence were then used to estimate the nonlinear response values. The remaining values were used for out of sample statistical testing of the quality of the characterisation of the differential equations. That is, the accuracy with which the estimated response function values can describe the behaviour of the process was determined by the normalised root mean square (nrms) difference between the actual data sequences $\{x(t)\}$ and the out of sample forecast $\{x_f(t)\}$ is

$$\text{nrms} = \sqrt{\frac{1}{\Lambda}\sum_{t=1}^{\Lambda}\left(\frac{x(t) - x_f(t)}{x(t)}\right)^2} \qquad (13)$$

where Λ denotes the sample length, and where f denotes the out of sample forecast in this case.

The solution of the Lorentz equations was assumed to be of the form

$$\phi_{u_v}(t) = \Xi_u(t) + \theta_{u_v}(t)$$

$$= \Xi_u(t) + \sum_{n=1}^{N} \frac{1}{n!} \sum_{i_1=1}^{M} \cdots \sum_{i_n=i_n-1\sigma_1=0}^{M} \sum_{\sigma_n=0}^{\mu} \cdots \sum_{\sigma_n=0}^{\mu} h_{\phi_{u_v}\Phi_{i_1}\ldots\Phi_{i_n}}(\sigma_1,\ldots,\sigma_n)$$

$$\prod_{j=1}^{n} \left\{\Phi_{i_j}(t-\sigma_j) - \Xi_{i_j}(t-\sigma_j)\right\} \delta\left(u_v \neq i_j;\ u_v = i_j\ \sigma_j > 0\ \ j=1,\ldots,n\right)$$

with N=2, μ=1 and M=3.

The coefficients estimated using the moment hierarchy method for the case where the addative noise with a variance of 0.001, which is typical of the value used in the recent literature, are shown in Table 1.

Table 1: Estimated coefficients of the differential equations from the noisy data

term	$\frac{dx_1}{dt}$ actual	$\frac{dx_1}{dt}$ estimated	$\frac{dx_2}{dt}$ actual	$\frac{dx_2}{dt}$ estimated	$\frac{dx_3}{dt}$ actual	$\frac{dx_3}{dt}$ estimated
x1	-10.0	-9.99970	100.80	100.797	0.0	-0.656×10^{-3}
x2	10.0	9.99995	-1.00	-1.00045	0.0	-0.114×10^{-4}
x3	0.0	-0.164×10^{-4}	0.0	0.273×10^{-4}	-2.67	-2.66639
x1x1	0.0	0.1777×10^{-5}	0.0	0.197×10^{-4}	0.0	0.0
x1x2	0.0	0.0	0.0	0.0	0.0	0.0
x1x3	0.0	0.0	0.0	0.0	0.0	0.0
x2x1	0.0	0.904×10^{-5}	0.0	-0.686×10^{-5}	1.0	0.99998
x2x2	0.0	0.444×10^{-5}	0.0	0.152×10^{-4}	0.0	0.154×10^{-4}
x2x3	0.0	0.0	0.0	0.0	0.0	0.0
x3x1	0.0	-0.298×10^{-5}	-1.00	-0.99978	0.0	0.411×10^{-5}
x3x2	0.0	0.851×10^{-6}	0.0	0.232×10^{-5}	0.0	0.975×10^{-5}
x3x3	0.0	0.284×10^{-6}	0.0	-0.164×10^{-5}	0.0	-0.320×10^{-5}

Ignoring the effect of terms with coefficients with values less than the value of the variance of the noise estimated using equation (10), and rounding to three decimal places, the reconstructed differential equations are

$$\frac{dx_1}{dt} = -10.000x_1 + 10.000x_2$$

$$\frac{dx_2}{dt} = -x_1x_3 + 100.797x_1 - x_2$$

$$\frac{dx_3}{dt} = x_1x_2 - 2.666x_3$$

As can be seen the moment hierarchy has correctly and accurately reconstructed the coupled ordinary differential equations in the presence of noise. It should be emphasised that all of the nonlinear response values are simultaneously determined in the analysis.

Figure 1 shows the effect of additive Gaussian random noise on the estimated coefficient values. As can be seen the estimated coefficient values remain robust, accurate and consistent up to significant contributions from additive noise.

In order to test the predictive ability of the model coefficients two sequences of data were generated using the same initial condition, one sequence is generated using the estimated response values and the other sequence generated using the actual response values. Figure 2 shows a sample of the forecast values $\{x_p(t)\}$ together with the observed sequence of data $\{x(t)\}$ for the noiseless case. The forecasts are of the 'runaway' type rather than the 'read-correct' type, in that the initial conditions are selected and the forecast is continued without knowledge of the actual data values for a reasonable duration or until 'blow-up' occurs. There is no observable difference between the two sequences shown in Fighre 2. In order to see the temporal development of the divergence between $\{x_p(t)\}$ and $\{x(t)\}$, Figure 3 shows a plot of the common logarithm of the absolute difference between the two series, i.e. $\left|x(t) - x_p(t)\right|$, is given.In Figure 3 it can be seen the divergence is exponential until the amplitude of the differences is the same as the envelope of $\{x(t)\}$ when the limit of forward prediction has been reached. The gradient of the diverging difference is related to the Lyapunov exponent. Thus the moment hierarchy has accurately identified the correct values and form of the nonlinear mapping. The response values estimated from the data are able to predict the future time series values for a duration defined by the intersection of the Lyapunov curve with the envelope of time series sequence, and with a precision that is dependent on the Lyapunov exponent of the initial value problem. In practice the value of μ and the order N have to be determined in the analysis and may be considered as free parameters. The order can be identified from a plot of $\{x(t)\}$ with $\{x_p(t)\}$ for deviations from a straight line which can indicate the presence of higher order terms.

An empirical model of the behaviour of the fof2 ionospheric peak intensity

As the solar wind impacts the earth's bow shock some of the particles enter the magnetopause, the boundary between the open magnetic field of the solar wind and the closed magnetic field of the earth. The manner in which these high energy particles enter and interact with the earth's upper atmosphere remains one of the outstanding problems of space science. The ionosphere is that part of the earth's upper atmosphere where the plasma density is sufficiently great that it can affect the propagation of radio waves.

The plasma is produced by the daytime ionisation of molecules irradiated with electromagnetic radiation from the sun and by the high energy particles from the solar wind near to the magnetic poles. The peak in the ionoshperic plasma occurs between 80 km and 300km in the so called F region, the maximum plasma density of which is denoted as fof2. Ionospheric transport is due to both non-electromagnetic forces (the atmospheric wind) and electromagnetic forces which, at high latitudes, produce plasma drift velocities in the range 0.2 km/sec to 2 km/sec.

The main effect of these drift velocities is to change the height and maximum particle density of the F layer which has consequential effects on communication and electromagnetic propagation. The lifetimes before recombination of the ions in the F region plasma are typically a few hours, although this is variable depending on the temperature and ion density as functions of height and time. During this time the ions can be transported for thousands of kilometres, consequently the ions form a weak plasma that has a highly complex spatio-temporal distribution.

There are a number of steady state empirical models which characterise the steady state periodic behaviour of the peak intensity and altitude of the F and E ionospheric layers used for communications. The main advantage of these models is their computational efficiency and their main disadvantages are their spatial sparseness and they cannot describe the dynamical behaviour observed in the ionosphere.

The empirical model developed here can accurately describe and predict the observed dynamic behaviour of the fof2 peak density of the ionosphere during equilibrium and nonequlibrium periods throughout the year, in both high and low sunspot activity years. The predicted future behaviour of the ionosphere can be used to constrain the boundary conditions of a numerical calculation procedure.

This allows the spatial and temporal behaviour of the ionosphere around the globe to be predicted, hence forthcoming propagation effects can be corrected for and knowledge of the physical processes studied with more realism in more detail.

In the present example analysis, the maximum frequency, its rate of change and rate of acceleration of that electromagnetic communications can be propagated through the ionospheric F layer at any particular time is defined by the discrete Volterra functional expansion truncated to order N, defined by the simultaneous equations

$$x_u(t) = \sum_{n=1}^{N} \frac{1}{n!} \sum_{i_1=1}^{M} \cdots \sum_{i_n=i_{n-1}\sigma_1=0}^{M} \sum_{\sigma_n=0}^{\mu} \cdots \sum_{\sigma_n=0}^{\mu} h_{x_u \Phi_{i_1} \cdots \Phi_{i_n}}(\sigma_1,\ldots,\sigma_n) \prod_{j=1}^{n} \Phi_{i_j}(t-\sigma_j) \tag{14}$$

$$\frac{dx_u(t)}{dt} = \sum_{n=1}^{N} \frac{1}{n!} \sum_{i_1=1}^{M} \cdots \sum_{i_n=i_{n-1}\sigma_1=0}^{M} \sum_{\sigma_n=0}^{\mu} \cdots \sum_{\sigma_n=0}^{\mu} h_{\frac{dx_u}{dt} \Phi_{i_1} \cdots \Phi_{i_n}}(\sigma_1,\ldots,\sigma_n) \prod_{j=1}^{n} \Phi_{i_j}(t-\sigma_j) \tag{15}$$

$$\frac{d^2x_u(t)}{dt^2} = \sum_{n=1}^{N} \frac{1}{n!} \sum_{i_1=1}^{M} \cdots \sum_{i_n=i_{n-1}\sigma_1=0}^{M} \sum_{\sigma_n=0}^{\mu} \cdots \sum_{\sigma_n=0}^{\mu} h_{\frac{d^2x_u}{dt^2} \Phi_{i_1} \cdots \Phi_{i_n}}(\sigma_1,\ldots,\sigma_n) \prod_{j=1}^{n} \Phi_{i_j}(t-\sigma_j) \tag{16}$$

where N=2 is the order of truncation of the Volterra functional expansion, T=2 is the highest order of temporal derivative considered, M is the number of ionosonde stations included in the analysis and varies between 6 and 30, t denotes time and the σ_js denote time delay with respect to the time t. Here the elements $\Phi_{i_j}(t)$ are drawn from the set of ionosonde measurements and their temporal derivatives given by

$$\{\Phi_i(t)\} = \left\{ x_1,\ldots x_M, \frac{dx_1}{dt},\ldots,\frac{dx_M}{dt},\ldots,\frac{d^T x_1}{dt^T},\ldots,\frac{d^T x_M}{dt^T} \right\}.$$

The values for the temporal derivatives were approximated by finite differences of adjacent points in each sequence of time series data. The ascending order auto- and cross- time series moments of the data and temporal derivatives were calculated and substituted into the moment hierarchy given by equation (9) with N=2 and μ=1. The moment hierarchy was then inverted to solve for the unknown response function values, which are also the coefficients of the governing differential equations in this case. Missing data values were replaced with the value from 72 hours previously.

Approximately 15 days of hourly ionosnde data were used to estimate the time series moments of the data and a grid search enabled the value of the variance of $\{\Xi_k(t)\}$ to be estimated simultaneously with the empirical coefficients of the governing differential equations given by equations (14), (15) and (16) for this example analysis. Figures 4 and 5

shows typical out of sample rolling coupled forecast with their associated uncertainties for several of the ionosonde stations in the coupled analysis in the northern hemisphere during the equinox periods of high and low sunspot years. Figures 6 shows typical out of sample rolling coupled forecast with their associated uncertainties for six ionosonde stations used in the coupled analysis during the equinox period of a high sunspot year.

Superimposed on each predictions is the sequence of actual ionosnde values with their uncertainties. Clearly the agreement is good within the statistical uncertainties for each prediction. The example of coupled analysis presented here provides good predictions for about 99% of the 300 by 3 day out of sample predictions of f0f2 value using the moment hierarchy defined by equations (9). A detailed exposition of an ongoing study of ionospheric data using different N and μ values in equation (9) is to be presented elsewhere.

Conclusions

The results presented in this paper can be summarised as follows. A new method has been presented which can extract the coefficients of mixed linear-nonlinear coupled differential equations from multivariate time series data. The discrete time theoretical representation is based on a truncated order Volterra functional series. The solution of the coupled differential equations was considered to be a vector field. This field being a function of the underlying physical observables, and for example, the ionosonde fof2 maximum frequency for electromagnetic communications through the ionosphere. The time series data observed from physical processes are, in almost all practical cases, discrete even though the attributes of the data are often modelled by continuous processes. Thus in this work a discrete approximation to the multi-dimensional Volterra functionals was used. A tractable set of simultaneous equations with well behaved coefficients can be generated by taking time series moments of a suitably truncated Volterra series expansion. This moment hierarchy was solved for the unknown differential equation coefficients using linear algebra. The kernel, or response, functions, of the Volterra functional expansion represent the dynamic behaviour of the physical process.

Observations can only be made with a finite precision and the mathematical model used to represent the physical process should take account of this inherent uncertainty. The effects of noise and measurement uncertainty were included in the representation and data analysis procedure.

Two example analyses were presented. A numerical example using the Lorentz equations demonstrated the ability and accuracy with which the coefficients were estimated from vector time series sequences in the presence of additive Gaussian noise. The second example considered the global prediction of the fof2 maximum communication transmission frequency in the ionosphere. Typical results from an in depth study were presented and the representation was shown to provide accurate and consistent predictions of future behaviour for a wide range of ionospheric conditions. This is the first accurate and consistent empirical dynamic model of the ionosphere to be developed. Detailed findings from that ongoing study will be presented elsewhere.

Acknowledgments

The authors would like to acknowledge that the work for the analysis of the fof2 data was funded in part by the U.K. Department of Trade and Industry. The authors would like to thank Mike Lockwood and John Norbury for their helpful discussions regarding this analysis.

References

[1] Volterra V., ***Theory of Functionals and of Integral and Integro-differential Equations***, Dover, New York, 1959.

[2] Dewson T. and Irving A. D., Linear and non-linear response function estimation from multi-input systems, To appear in ***Physica D***, 1996.

[3] Irving A. D., Dewson T., Hong G. and Cunliffe N. H., General nonlinear response of a single input system to stochastic excitations, ***Applied Mathematical Modelling***, Vol. 19, 1995, pp 45-56.

[4] Irving A. D., Clayton B. R. and Dewson T., Nonlinear thermoviscoelastic behaviour in complex materials , ***IUTAM Symposium on Inhomogenity, Anisotropy and Nonlinearity in Solid Mechanics***, Elsevier, 1995, pp 125-132.

[5] Irving A. D., Stochastic Sensitivity Analysis, ***Applied Mathematical Modelling***, Vol. 16, 1992, p1-12.

[6] Irving A. D. and Dewson T., General mixed linear-nonlinear response of evolutionary causal physical processes, ***In Preparation***.

[7] Broomhead D. S., Jones R. and King G. P., ***J. Phys. A***, 20, 1987, L563.

[8] Broomhead D. S. and King G. P., Extracting quantitative dynamics from experimental data, ***Physica D***, 20, 1986, pp 217-236.

[9] Casdagli M., Nonlinear prediction of chaotic time series, ***Physica D***, 35, 1989, pp 335-356.

[10] Farmer J. D. and Sidovowich J. J., Predicting chaotic time series, ***Phys. Rev. Lett.***, 59, 1987, pp 845-848.

[11] Crutchfield J. P. and McNamra B. S., Equations of motion from a data series, ***Complex Systems***, 1, 1987, pp 417-452.

[12] Cremers J. and Hubler A., Construction of differential equations from experimental data, ***Z. Naturforsch A***, 42, 1986, pp 797-802.

[13] Gouesbet G., Reconstruction of the vector fields of continuous dynamical systems from scalar time series data, ***Phys. Rev. A***, 43, 1991, pp 521-.

[14] Rowlands G. and Sprott J. C., Extraction of dynamical equations from chaotic data, ***Physica D***, 58, 1992, pp 251-259.

[15] Gonesbet G. and Maquet J., Construction of phenomenological models from numerical scalar time series, ***Physica D***, **58**, 1992, pp 202-215.

[16] Bunimovich L. A., Coupled map lattices: one step forward and two steps back, ***Physica D***, 86, 1995, pp 248-255.

[17] Irving A. D. and Dewson T., The analysis of complex times series data, ***Applied Mathematical Modelling***, Vol. 20, 1996, pp 35-47.

[18] Bittencourt J. A. and Chryssafidis, Comparison of IRI model predictions with low ionospheric observations, ***Adv. Space Sci.***, Vol 11, No. 10, 1991, pp 97-100.

[19] Rawer K., Ionospheric mapping in the polar and equatorial zones, ***Adv. Space Sci.***, Vol. 16, No. 1, 1995. pp 9-12.

[20] Besprogvannaya A. S., Empirical modelling of the F2 peak at 50-70 invariant lattitude using magnetic congujacy, ***Adv. Space Sci.***, Vol 11, No. 10, 1991, pp 23-28.

Figure captions

Figure 1. The estimated coefficients of the Lorentz equations as a function of additive Gaussian white noise.

Figure 2. An out of sample forecast of the solution of the Lorentz equations using the values of the coefficients estimated with the moment hierarchy method. Superimposed on the plot are the actual solution values which cannot be resolved from the estimated values.

Figure 3. The absolute difference values between the forecasted and actual solution values.

Figure 4. A number of out of sample forecasts of the fof2 maximum frequency for electromagnetic communication in the ionosphere for the ionosnde stations at Port Argiello, Slough and Novosibirsk in the northern hemisphere during a sunspot maximum year.

Figure 5. A number of out of sample forecasts of the fof2 maximum frequency for electromagnetic communication in the ionosphere for the ionosnde stations at Port Argiello, Slough and Novosibirsk in the northern hemisphere during a sunspot minimum year.

Figure 6. An out of sample forecast of the fof2 maximum frequency for electromagnetic communication in the ionosphere for the ionosnde stations at Argentina Island, Brisbane, Hobart, Johannesburgh, Port Stanley and Tahiti in the southern hemisphere during a sunspot maximum year.

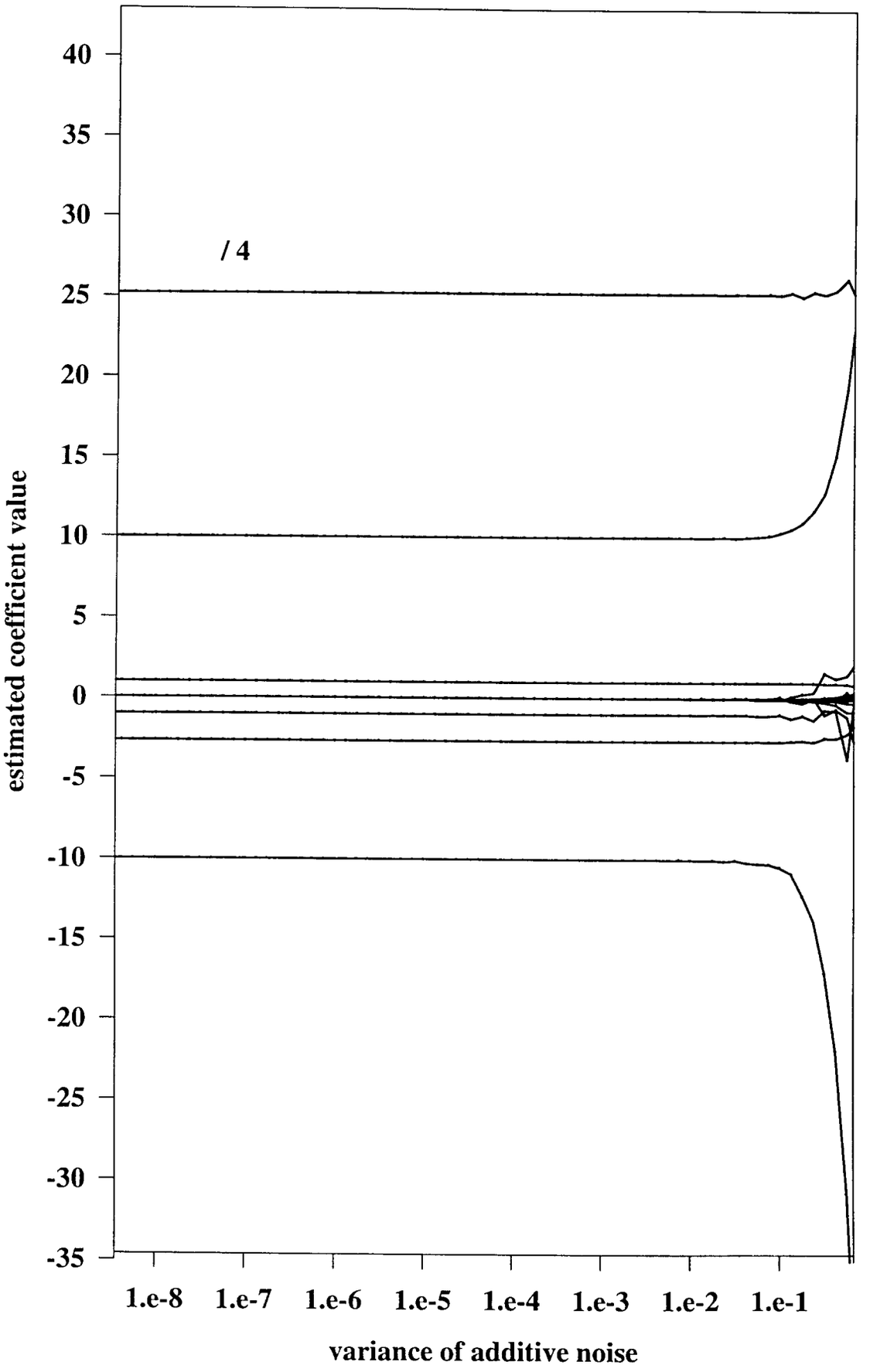
40
35
30
/ 4
25
20
15
10
5
0
-5
-10
-15
-20
-25
-30
-35
estimated coefficient value
1.e-8
1.e-7
1.e-6
1.e-5
1.e-4
1.e-3
1.e-2
1.e-1
variance of additive noise

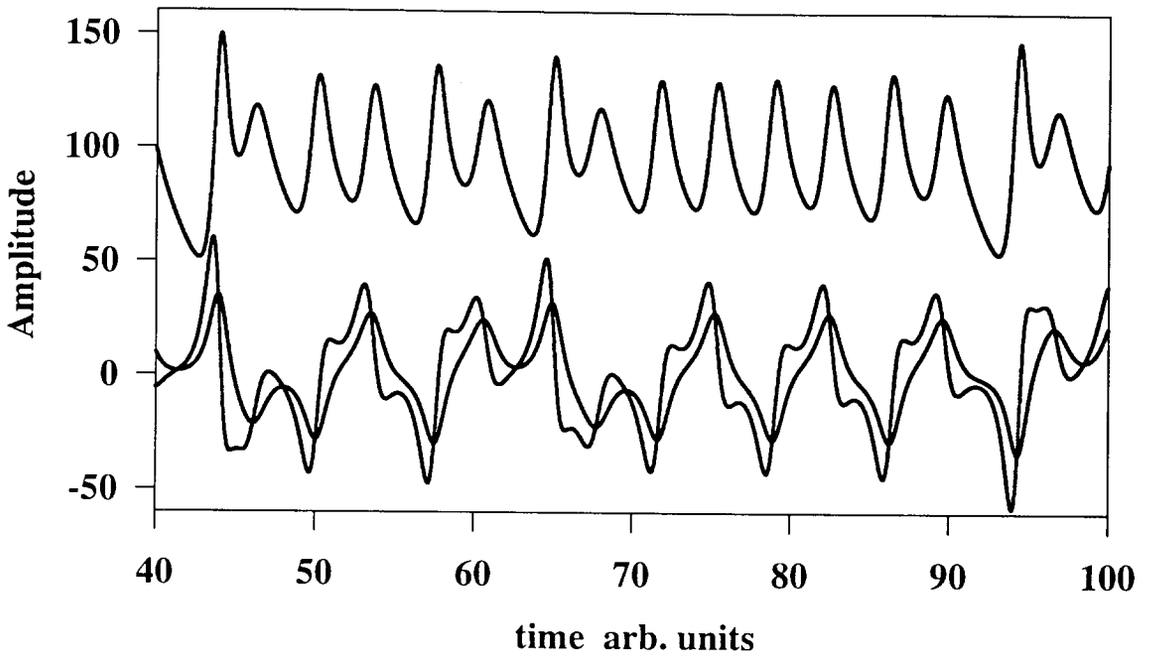
150
100
50
0
-50
Amplitude
40
50
60
70
80
90
100
time arb. units

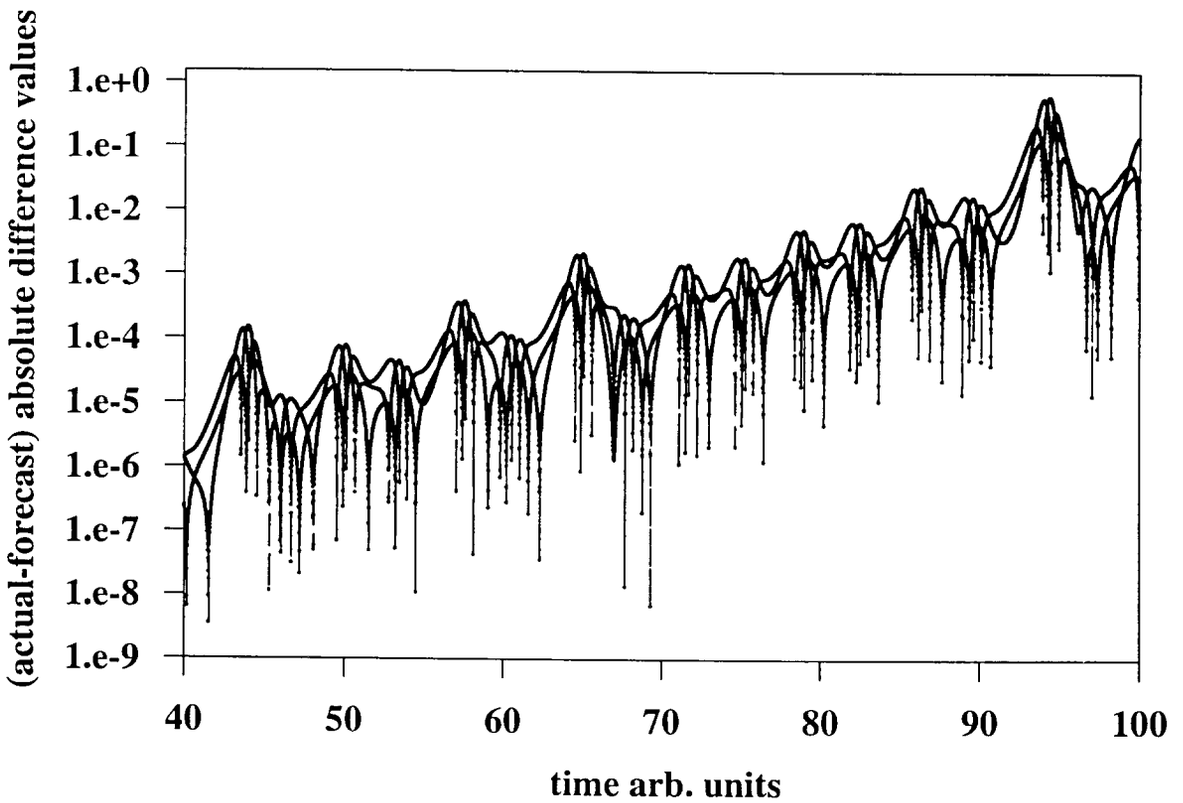
1.e+0
1.e-1
1.e-2
1.e-3
1.e-4
1.e-5
1.e-6
1.e-7
1.e-8
1.e-9
(actual-forecast) absolute difference values
40
50
60
70
80
90
100
time arb. units

Port Argiello from March 17 1980

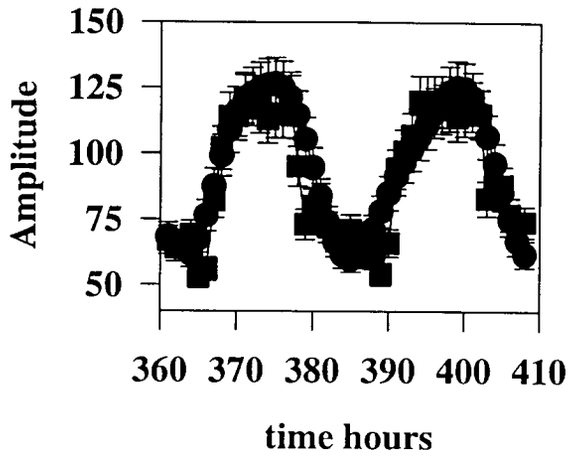

Point Argiello from September 17 1980

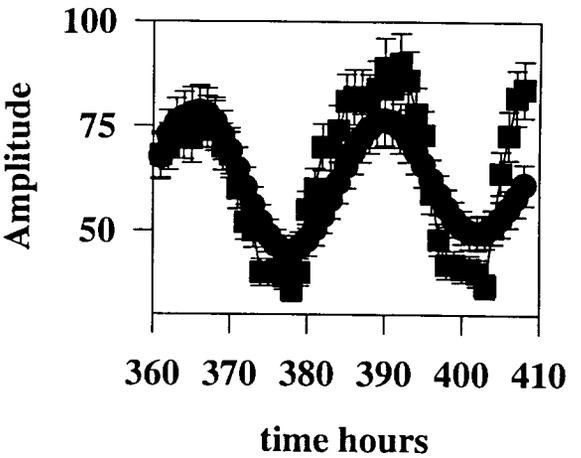

Slough from March 17 1980

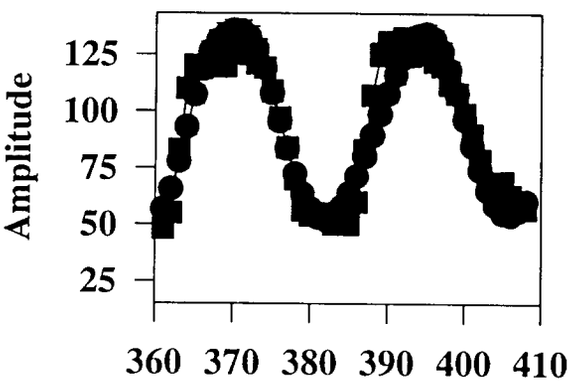

Slough from September 17 1980

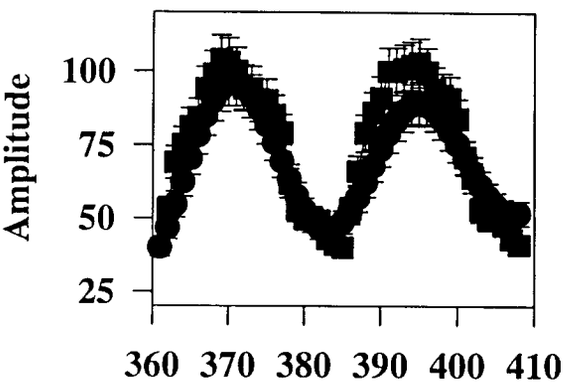

Novosibirsk from March 17 1980

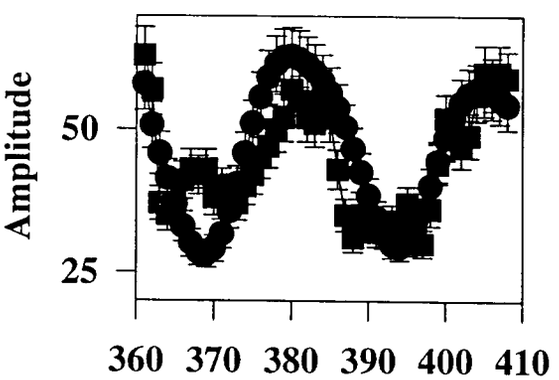

Novosibirsk from September 17 1980

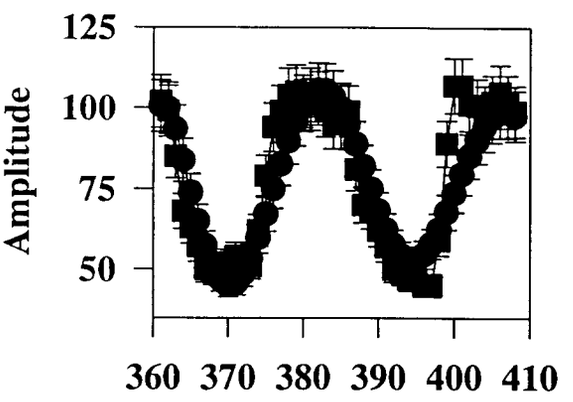

Port Argiello from March 17 1986

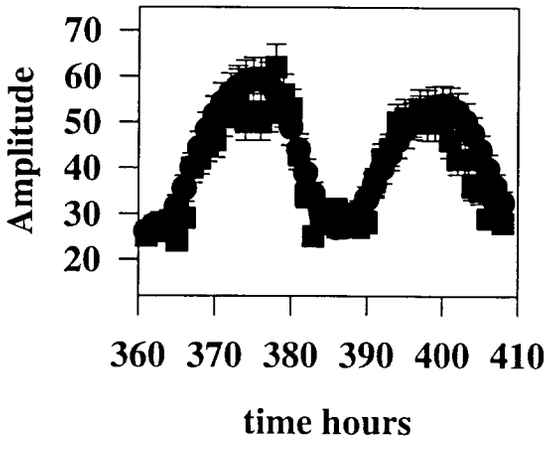

Point Argiello from September 17 1986

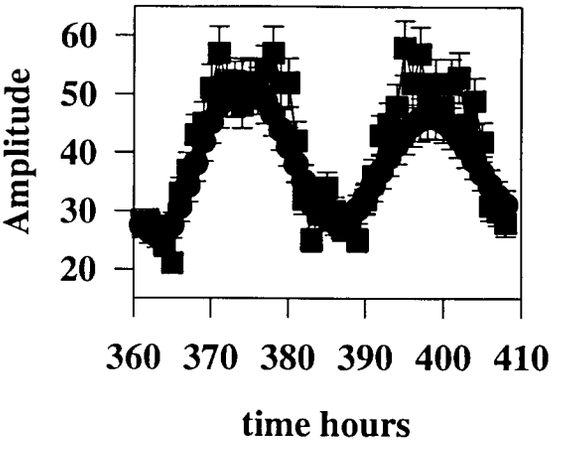

Slough from March 17 1986

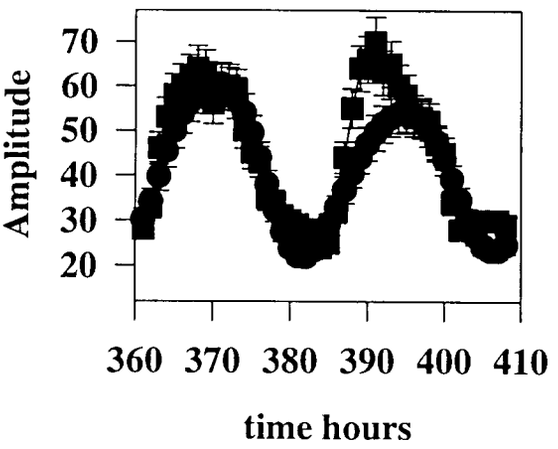

Slough from September 17 1986

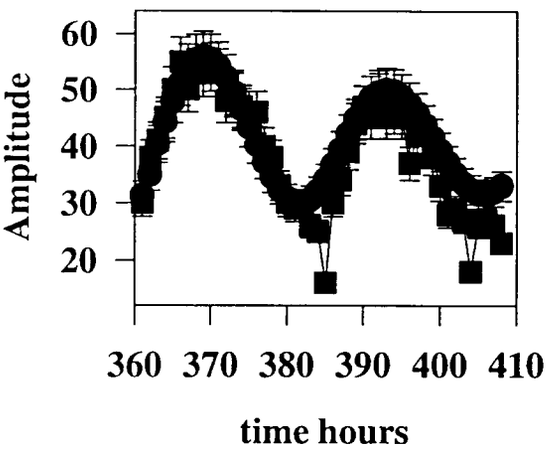

Novosibirsk from March 17 1986

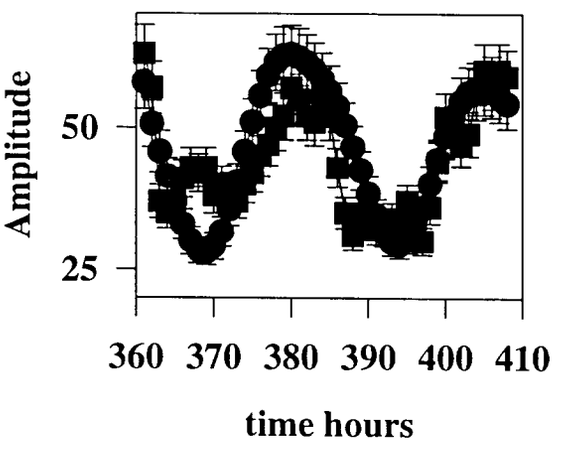

Novosibirsk from September 17 1986

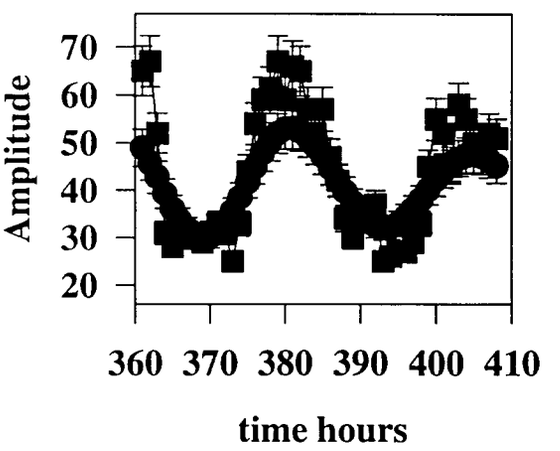

Argentina Island from March 17 1980

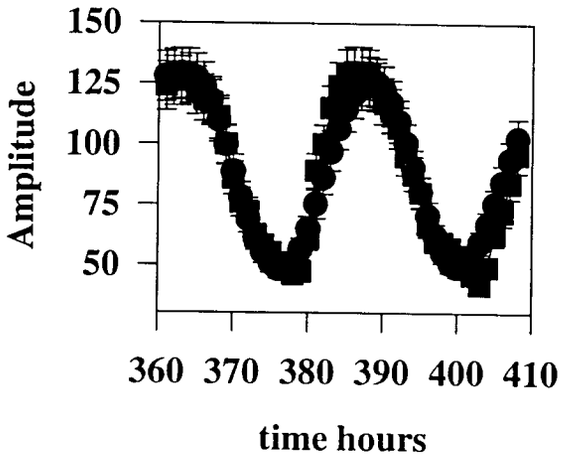

Johannesburg from March 17 1980

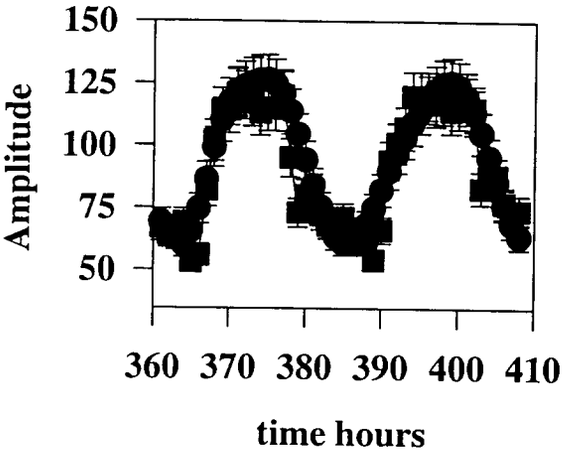

Brisbane from March 17 1980

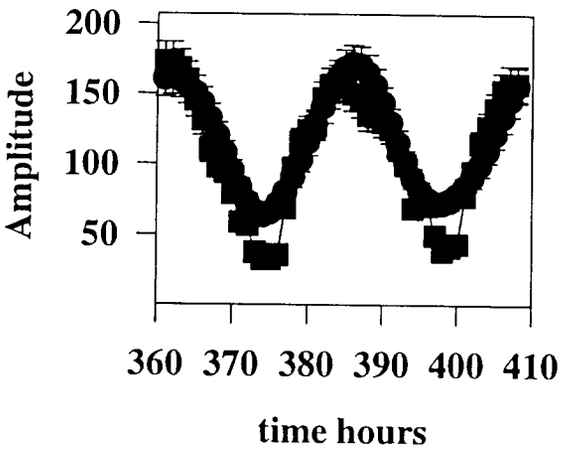

Port Stanley from March 17 1980

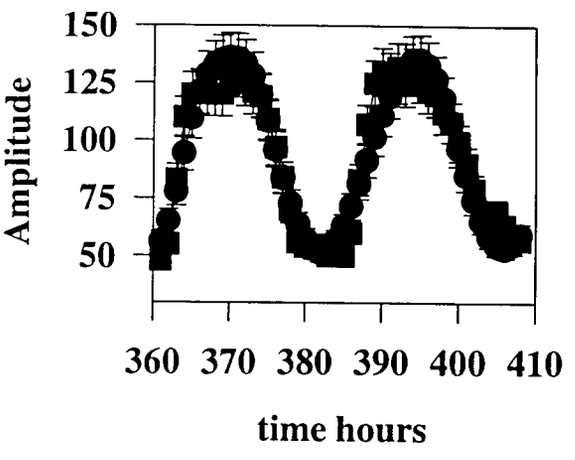

Hobart from March 17 1980

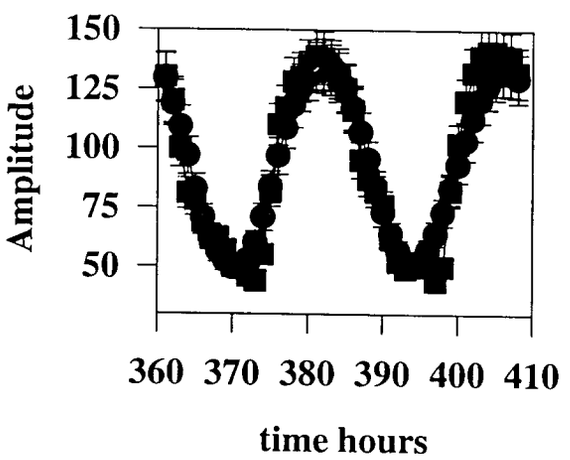

Tahiti from March 17 1980